Int. J. Electrochem. Sci., 12 **(2017)** 5363 – 5377, doi: 10.20964/2017.06.63

International Journal of ELECTROCHEMICAL SCIENCE
www.electrochemsci.org

Effect of Tempers on Electrochemical Corrosion Behavior of 7150 Aluminum Alloy Plate in Various Corrosive Media

Qingqing Sun[1,2,3], *Jiugang Hu*[1], *Jie Li*[1,*], *Kanghua Chen*[2], *Pengxuan Dong*[2], *Xingzhi Liao*[2], *Yang Yang*[3]

[1] School of Chemistry and Chemical Engineering, Central South University, Changsha 410083, Hunan, China
[2] State Key Laboratory of Powder Metallurgy, Central South University, Changsha 410083, Hunan, China
[3] School of Chemical Engineering, Purdue University, West Lafayette 47907, IN, USA
[*]E-mail: lijieliu@csu.edu.cn

Received: 31 May 2016 / *Accepted:* 13 April 2017 / *Published:* 12 May 2017

The effect of various tempers (peak ageing T6, RRA T77, two-step ageing T76, and a novel three-step ageing T76 + T6) on electrochemical corrosion of 7150 Al alloy under three corrosive solutions has been investigated. Electrochemical results and corrosion morphologies show that the resistance to pitting corrosion, inter-granular corrosion (IGC) and exfoliation corrosion of alloys is in the following decreasing order: T76 + T6 > T76 > T77 > T6. As indicated by TEM, the corrosion behavior of each temper might depend on the size and spacing of grain boundary particles of alloys. Excellent consistence between electrochemical parameter and stress cracking corrosion resistance was observed. In addition, the pit transition potential and potential differences as criteria to assess Al alloy corrosion behavior were also discussed.

Keywords: 7150 Al alloy; Temper; Cyclic polarization; Potential; TEM

1. INTRODUCTION

7000 series aluminum alloys are extensively used in aeronautical applications, due to their very low density, high strength and good toughness properties [1-3]. One limitation of their use in the metallurgical state of highest strength (commonly called T6 temper) is the low corrosion resistance under service environment. T7x over-aged temper increases the corrosion resistance at the expense of 10–15% strength [4, 5]. For the purpose of achieving a good combination between strength and corrosion properties, many efforts have been carried out. Retrogression and re-aging (RRA), first proposed by Cina [6], can increase corrosion resistance of 7000 series Al alloy while keep the strength levels similar to T6 aged alloy. This type of heat treatment comprises first an ageing step, leading to an under-aged or a T6 state. Retrogression treatment of alloy is performed under short duration at high temperature, dissolving part of the initially formed precipitates. Finally, a third-step like the first one, leads to the final microstructure. Peng et al. [7] reported that the repetitious-RRA (DRRA) could further improve stress cracking corrosion resistance of Al-Zn-Mg-Cu alloy. However, the retrogression treatment of RRA and repetitious-RRA in the range of 180 ~ 260 °C lasting for several minutes is too short, which is difficult to apply on thick Al plates in industry [8, 9]. This is due to that thermal gradients between the surface and intermediate layer of thick plates would result in residual stress problem. For many cases, residual stress plays an important role in distortion or cracking. Therefore, it is of great significance to find new ageing processes that can control residual stress magnitudes for the thick Al plate. Recently, a novel three-step aging has been proposed for Al-Zn-Mg-Cu thick plate [10]. This three-step ageing is similar with RRA, except that the second step ageing is under treated for longer duration at lower temperature, which would reduce the thermal gradients between alloy surface and the interior, thus solving the residual stress problem. It is indicated that this novel three-step ageing increases strength combination with fracture toughness of Al alloy, but there is few published work to study its corrosion performance.

Al alloys immersed in different corrosive media might have different corrosion behaviors and mechanisms, therefore it's necessary to select proper solutions for the thorough study of alloy corrosion. The purpose of the paper is to investigate and compare the influence of tempers (peak aged T6, RRA T77, over-aged T76, and three-step aged T76 + T6) on electrochemical corrosion of 7150 Al alloy plate under various corrosive media, as well as to report the suitability and limitations of some electrochemical parameters such as pit transition potential and potential differences.

2. MATERIALS AND METHODS

2.1. Alloys and heat treatments

The investigated material was a 7150 aluminum alloy plate received from Aluminum Corporation of China. The chemical composition of the plate is Al-6.2Zn-2.3Mg-2.2Cu-0.15Zr-0.08Fe-0.061Si (mass fraction). The samples, cut into 15×15×3 mm plates, were solution heat treated for 30 min at 480 ℃, followed by water quenching. Then the samples were treated with four different ageing processes: peak ageing T6 (120 ^{0}C*24h, air cooling), RRA T77 (120 ^{0}C*24h, air cooling + 180 ^{0}C*0.5h, water cooling + 120 ^{0}C*24h, air cooling), two-step ageing T76 (120 ^{0}C*24h, air cooling + 160 ^{0}C*8h, water cooling), and a novel three-step ageing T76 + T6 (120 ^{0}C*24h, air cooling + 160 ^{0}C*8h, water cooling + 120 ^{0}C*24h, air cooling).

2.2. Electrochemical measurements

For electrochemical characterization, samples were wet ground through successive grades of silicon carbide abrasive papers from P400 to P2000, followed by diamond finishing to 0.1 μm. A CHI

660C electrochemical workstation (3700 Tennison Hill Drive1 Austin, TX787381, USA) connected to a three-electrode cell was used for the electrochemical measurements. The working electrode was the test material with an immersed area of 0.5 cm^2 and platinum plate and saturated calomel (SCE) electrodes were used as the counter and reference electrodes, respectively. The test solutions were aerated 3.5 wt % NaCl、20 mmol/L NaCl + 0.1 mol/L Na_2SO_4 and 4 mol/L NaCl + 0.5 mol/L KNO_3 + 0.1 mol/L HNO_3 (EXCO) solutions. Open circuit potential (OCP) curves of 7150 Al plate were firstly performed. Then cyclic polarization curves were obtained at a scan rate of 1 mV/s, ranging from -1.2 to -0.4 V_{SCE} for 3.5 wt % NaCl and EXCO solutions and from -1.2 to -0.2 V_{SCE} for 20 mmol/L NaCl + 0.1 mol/L Na_2SO_4 solution. All electrochemical tests were conducted in a Faraday cage.

2.3 Hardness and conductivity

Vickers hardness was measured by loading 294 N with a HBRUV-187.5 instrument on the surface of specimens subjected to various ageing process. Electronic conductivity (% IACS—International Annealed Copper Standard) was measured by using a 7501A eddy current conductivity meter. Hardness and conductivity values are the mean values of at least five measurements.

2.4 Microstructure and corrosion morphology

Microstructures were characterized by optical microscopy and bright field imaging in a TECNAI G^2 20 TEM. The samples for optical microscopy were prepared by Graff-Sargent reagent. After cyclic polarization tests, the surfaces of investigated alloys were characterized by scanning electron microscopy (SEM) and optical morphology in order to study the morphology and mechanism of corrosion.

3. RESULTS

3.1 Optical microstructure

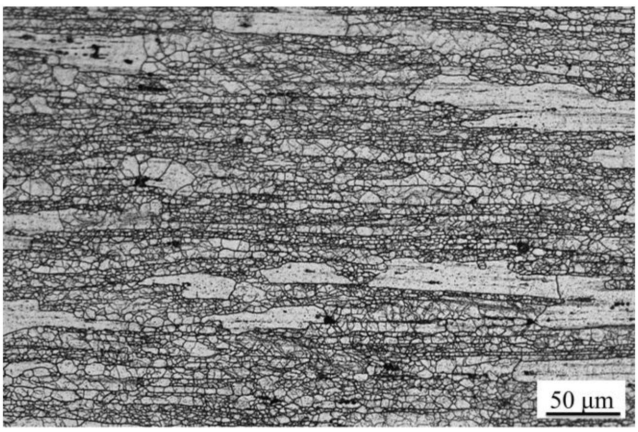

Figure 1. Optical microstructure of 7150 Al alloy plate

7150 Al plate exhibits partially recrystallized microstructure, as can be easily seen in Fig. 1. This kind of microstructure usually implies that the alloy is susceptible to localized corrosion, especially to intergranular corrosion and stress cracking corrosion [11, 12].

3.2 Open circuit potential

Open circuit potential curves of 7150 Al plate subjected to various tempers are shown in Fig. 2. Under all chosen solutions, peak aged T6 alloy has the lowest OCP value, indicating the highest corrosion sensitivity. OCP values of T77 and T76 aged alloys are close, which shows the proximity in corrosion susceptibility of these two alloys. By adding another T6 to over-aged T76, OCP of Al plate exhibited the most positive (anodic) amongst the four studied aged alloys, indicating the best corrosion resistance of it. It also should be noted that, OCP values of alloys in 20 mmol/L NaCl + 0.1 mol/L Na_2SO_4 solution is the most positive (~0.60 V_{SCE}), followed by 3.5 wt % NaCl solution (~0.70 V_{SCE}) and EXCO solution (~0.73 V_{SCE}). This suggests that the corrosion severity of solutions is in the following decreasing order: EXCO > 3.5 wt % NaCl > 20 mmol/L NaCl + 0.1 mol/L Na_2SO_4.

(a)

(b)

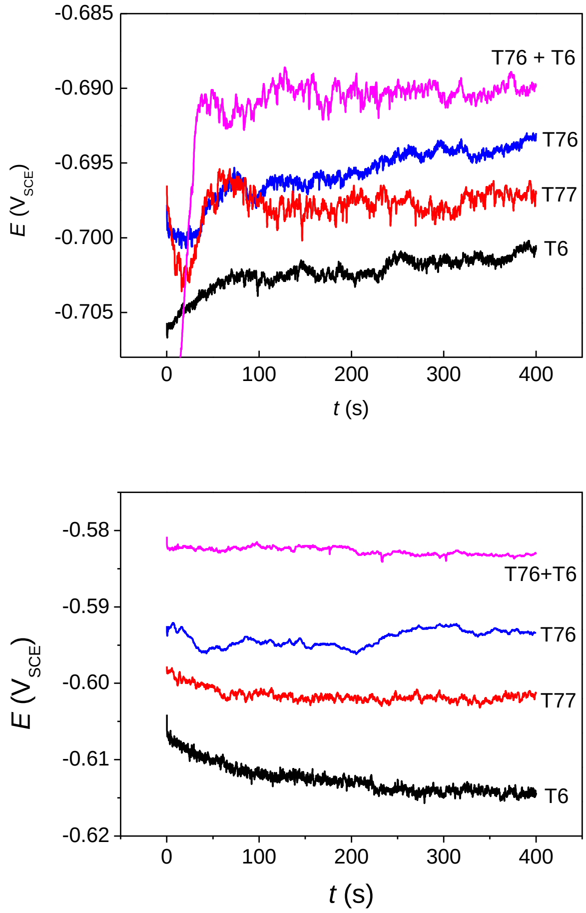

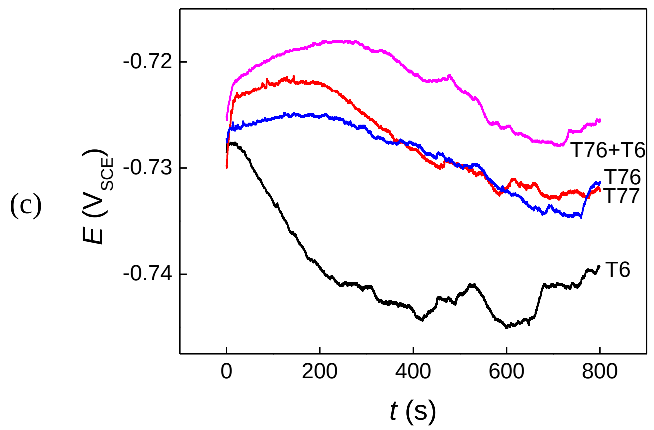

Figure 2. Open circuit potential curves of 7150 Al plate subjected to various ageing treatments under (a) 3.5 wt% NaCl solution, (b) 20 mmol/L NaCl + 0.1 mol/L Na_2SO_4 solution and (c) EXCO solution.

3.3 Cyclic polarization curves

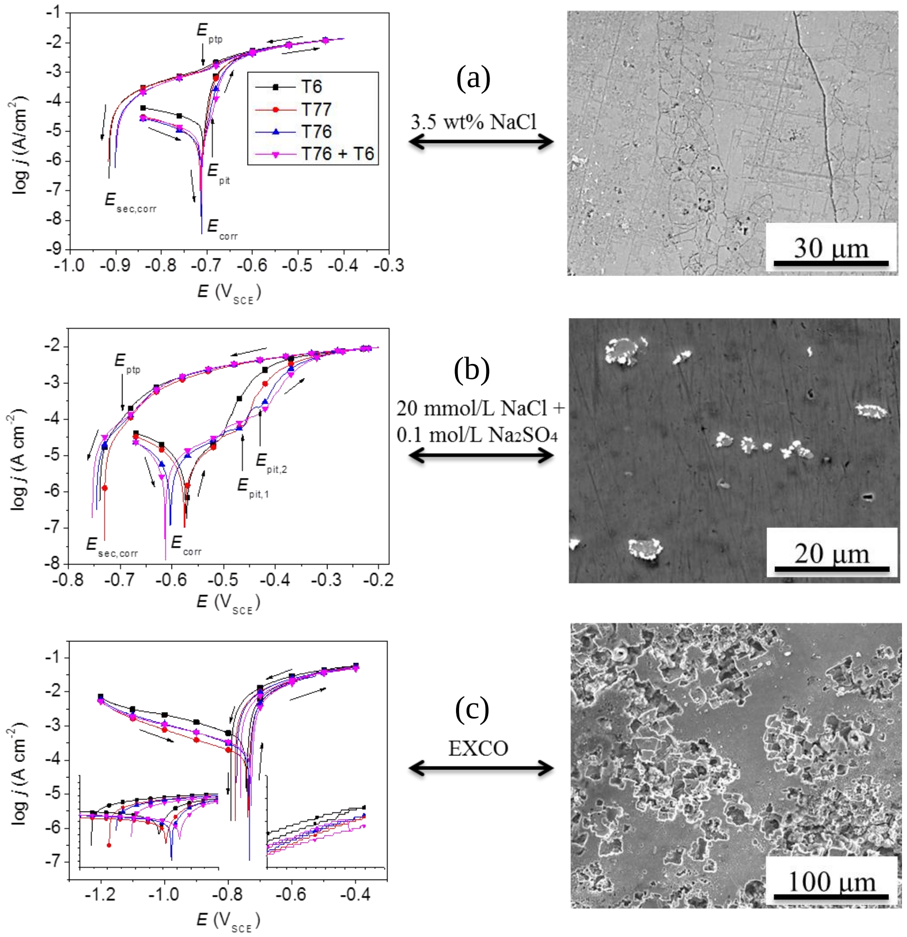

Figure 3. Cyclic polarization curves and SEM corrosion morphologies of 7150 Al plates subjected to different heat treatments in three corrosive electrolytes: (a) 3.5 wt % NaCl; (b) 20 mmol/L NaCl+0.1 mol/L Na_2SO_4; (c) EXCO

Cyclic polarization curves of 7150 Al alloy plate subjected to different tempers are depicted in Fig. 3. The selected corrosive media have different chloride concentrations and pH values, which lead to different shapes of cyclic polarization curves as well as different corrosion morphologies and mechanisms. For 3.5 wt% NaCl solution, intergranular corrosion and pitting corrosion are found on the surface of Al alloy (Fig. 3a). For 20 mmol/L NaCl + 0.1 mol/L Na_2SO_4 solution, only pits can be seen on the specimen surface, corresponding to the presence of obvious pitting potential in Tafel plots (Fig. 3b). For the severest solution, EXCO, exfoliation corrosion occurs (Fig. 3c).

Various electrochemical parameters can be derived from cyclic polarization curves. The parameters, including corrosion potential (E_{corr}), corrosion potential of the reverse scan ($E_{sec,corr}$), corrosion current densities (I_{corr}), linear polarization resistances (R_{corr}), first pitting potential ($E_{pit,1}$) and second pitting potential ($E_{pit,2}$), were listed in Table 1. Among the four studied tempers, T6 peak aged alloy shows the highest cathodic limit current density under the three corrosive media, respectively. In addition, compared to peak aged alloy, the rest alloys present lower corrosion current densities as well as higher linear polarization resistances, indicating slower corrosion rate obtained for the rest. In the solution of 20 mmol/L NaCl+0.1 mol/L Na_2SO_4, it can be seen that obvious pitting potentials showing up in cyclic polarization curves. The first pitting potential $E_{pit,1}$ corresponds to transient dissolution caused by attack of the fine hardening particles and the surrounding solid solution in a thin surface layer, and the second pitting potential $E_{pit,2}$ is associated with intergranular and selective grain attack [13]. The value of $E_{pit,2}$ is -0.503, -0.456, -0.430 and -0.419 V_{SCE} for T6, T77, T76 and T76 + T6 aged Al plate, respectively. This indicates that the resistance to pitting corrosion of the four aged alloys is in the following order: T6 < T77 < T76 < T76 + T6.

Table 1. Parameters of cyclic polarization curves in various media

medium	Ageing	E_{corr} V_{SCE}	I_{corr} A/cm^2	R_{corr} $\Omega\cdot cm^2$	$E_{sec,corr}$ V_{SCE}	$E_{pit,1}$ V_{SCE}	$E_{pit,2}$ V_{SCE}
3.5 wt % NaCl	T6	-0.708	2.08×10^{-5}	228	-0.914	/	/
	T77	-0.714	9.44×10^{-6}	264	-0.916	/	/
	T76	-0.712	7.64×10^{-6}	288	-0.901	/	/
	T76 + T6	-0.712	1.09×10^{-5}	400	-0.899	-0.691	/
20 mmol/L NaCl + 0.1 mol/L Na_2SO_4	T6	-0.572	4.69×10^{-6}	5636	-0.74	-0.503	/
	T77	-0.576	4.55×10^{-6}	7044	-0.731	-0.517	-0.456
	T76	-0.603	4.32×10^{-6}	6141	-0.746	-0.462	-0.43
	T76 + T6	-0.613	4.01×10^{-6}	5558	-0.754	-0.507	-0.419
EXCO	T6	-0.743	2.03×10^{-3}	26	-0.792	/	/
	T77	-0.738	1.05×10^{-3}	47	-0.779	/	/
	T76	-0.734	1.11×10^{-3}	34	-0.774	/	/
	T76 + T6	-0.728	1.02×10^{-3}	42	-0.763	/	/

Note the value listed here is the mean value of at least three tests

4. DISCUSSION

4.1 Corrosion potential and corrosion

Different with equilibrium potential, corrosion potential E_{corr} is the mixed potential of anodic branch and cathodic branch. The electron transfer reactions on anodic and cathodic branches are different reactions involved with different chemical species. The increase of anodic branch current density would lead E_{corr} shifts to the negative direction, while the increase of cathodic branch would lead E_{corr} shifts to the positive direction. Thus, strictly, E_{corr} cannot be used to assess corrosion performance of alloys [14, 15]. However, in some specific cases, E_{corr} can be used as an empirical criterion for assessing corrosion. From the OCP and Tafel results, we can conclude that the corrosion resistance order of the studied alloys is T6 < T77 < T76 < T76 + T6. So that in the case of 20 mmol/L NaCl+0.1 mol/L Na_2SO_4, as shown in Fig. 4, E_{corr} shows downward trend with corrosion resistance ability. But in the case of EXCO, conversely, E_{corr} shows upward trend with corrosion resistance ability. While in 3.5 wt % NaCl solution, using E_{corr} to assess corrosion properties is unreliable. It can be seen that the trend between E_{corr} and corrosion resistance is very interesting, and is directly related to the specific corrosive medium in which the alloys immersed.

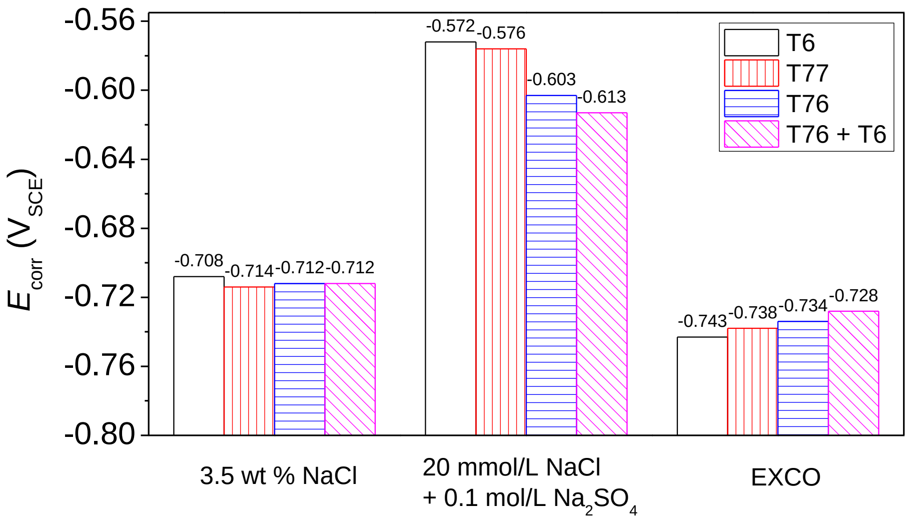

Figure 4. E_{corr} of 7150 Al plates subjected to different tempers under 3.5 wt% NaCl solution, 20 mmol/L NaCl + 0.1 mol/L Na_2SO_4 solution and EXCO solution

4.2 Pit transition potential and corrosion

Pit transition potential (E_{ptp}) corresponds to the inflection in the reverse portion of cyclic polarization curve, as shown in Fig. 5a. This characteristic parameter, was first reported by Yasuda [16], but didn't attract too much researchers' attention until recent years [17-20]. E_{ptp} was found to be independent of the surface state condition, changing little with the amount of corrosion, differently from E_{pit} and $E_{sec,corr}$ [18, 19]. The physical meaning of E_{ptp} still is very controversial. So many theories have been reported on this issue, e.g. one-dimensional tunnel theory [21], reactivation theory [20, 22], repassivation theory [23, 24], stepwise repassivation theory [16, 25] and even surface acidification theory [26]. Morrison [23] and Little [24] utilized E_{ptp} as the "protection potential" and "repassivation potential" to respectively assess the repassivation kinetics of $Zr_{41.2}Ti_{13.8}Ni_{10}Cu_{12.5}$Be22.5 metallic glass and Al–Cu–Mg–Ag alloys. Also it was reported that E_{ptp} decreased linearly as a function of the logarithm of chloride concentration [20], showing the suitability in corrosion assessment. Unfortunately, to our knowledge, few literatures have adopted E_{ptp} to evaluate corrosion behaviors. But, as can be seen in Fig. 3 and Fig. 5a, E_{ptp} is not as obvious as pitting potential, which makes it almost unreadable from the reverse portion of cyclic polarization curve. In order to accurately determine its value, the 1st derivative and the 2nd derivative curves of Fig. 5a are shown in Fig. 5b. As can be seen, E_{ptp} is the potential at the peak of the 2nd derivative curve. Cyclic polarization curves and the corresponding 2nd derivative curves of 7150 Al plates are shown in Fig. 6. Using this method, the values of E_{ptp} of 7150 Al plates in 3.5 wt % NaCl and 20 mmol/L NaCl+0.1 mol/L Na_2SO_4 solutions are presented in Fig. 7. For both of these two corrosion media, E_{ptp} trend as a function of ageing process is T6 < T77 < T76 < T76 + T6, which is exactly the same trend with corrosion resistance. This reconfirms the corrosion resistance order of the studied alloys subjected to different tempers. In addition, for each aged alloy, the E_{ptp} value in 3.5 wt % NaCl solution is higher than that of 20 mmol/L NaCl+0.1 mol/L Na_2SO_4 solution, which again proves the suitability of E_{ptp} for corrosion assessment of Al alloy.

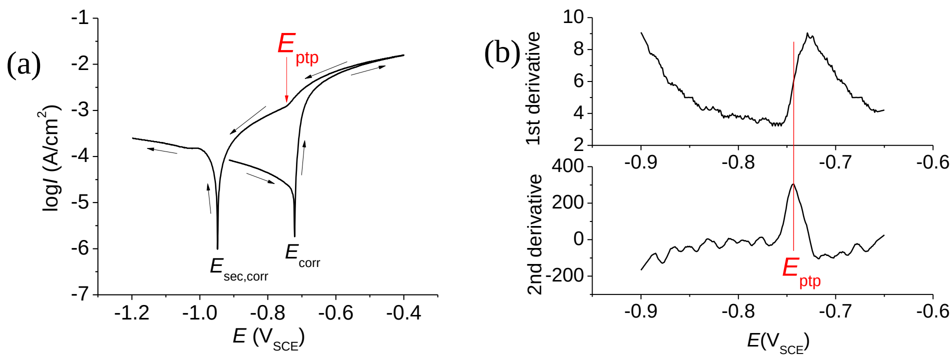

Figure 5. Cyclic polarization curve (a) and its 1st and 2nd derivative curves (b) of 7150 Al alloy plate

(a)

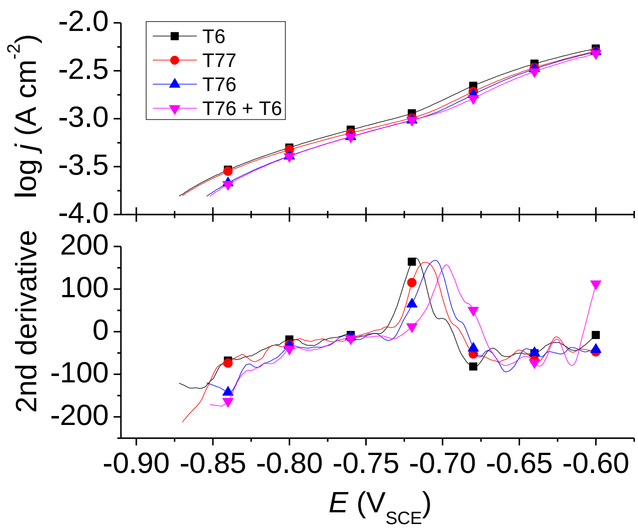

(b)

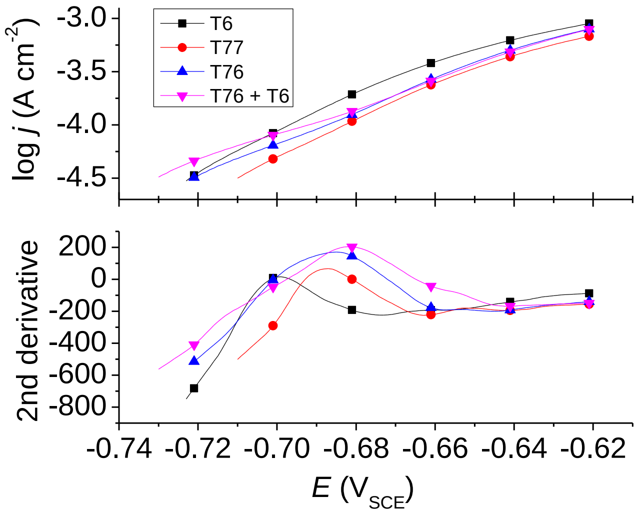

Figure 6. Cyclic polarization curves and the corresponding 2nd derivative curves of 7150 Al plates in (a) 3.5 wt % NaCl solution and (b) 20 mmol/L NaCl+0.1 mol/L Na_2SO_4 solution

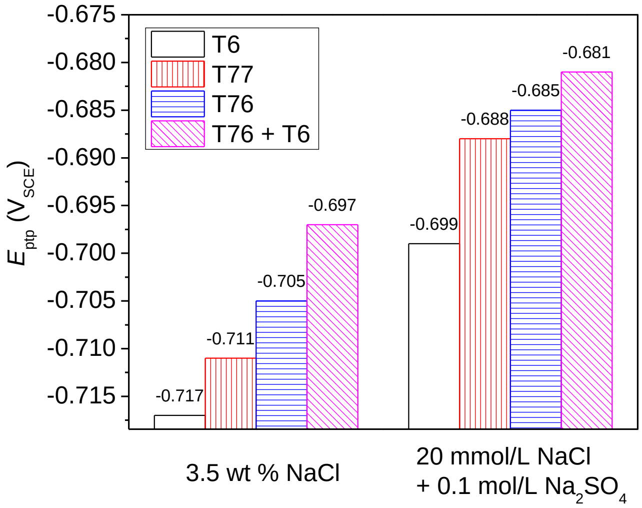

Figure 7. E_{ptp} values of 7150 Al plates in 3.5 wt % NaCl solution and 20 mmol/L NaCl+0.1 mol/L Na_2SO_4 solution

4.3 Potential differences and corrosion

Corrosion behavior and mechanism also can be reflected by ΔE ($E_{sec,corr} - E_{corr}$, $E_{pit} - E_{corr}$ and $E_{pit} - E_{sec,corr}$) trends, whose values are listed in Table 2. Potential differences as criteria have been used for several decades to predict localized corrosion susceptibility of alloys [19, 27-29]. Silverman [27, 28] proposed that, for a given experimental procedure, the higher the potential difference of $E_{sec,corr} - E_{corr}$ is, the harder certain metals can repassivate. As can be summarized from Table 2, for the three studied corrosive media, the values of $E_{sec,corr} - E_{corr}$ follows the following trend: T6 < T77 < T76 <

T76 + T6, which is consistent with the corrosion resistance trend. This shows good agreement with Silverman's proposal.

However, when we compared $E_{sec,corr} - E_{corr}$ values obtained from different solutions, the results challenged Silverman's proposal. The corrosion fraction of alloys after polarization tests were calculated using ImageJ2x software. Based on Silverman's proposal, it can be expected that the value of $E_{sec,corr} - E_{corr}$ should show monotonic decreasing trend with corrosion propagation. But unexpectedly, the value of $E_{sec,corr} - E_{corr}$ decreases firstly and then increases with the increasing of corrosion extent, as can be seen from Fig. 8. In addition, it should be noted that, based on our unpublished work, the general trend shown in Fig. 8 also was found when we change influencing factors like temperature, chloride concentration and point-of-reversal. This is probably due to corrosion mechanism change when immersing alloy in different corrosive media. These new findings revealed the limitations of using $E_{sec,corr} - E_{corr}$ for corrosion assessment. And further work is needed in order to fully understand the suitability and limitations of this extremely interesting parameter.

Table 2. ΔE values of cyclic polarization curves of alloys in various media

medium	Ageing	$E_{sec,corr}$ - E_{corr} V	E_{pit} - E_{corr} V	$E_{pit} - E_{sec,corr}$ V
3.5 wt % NaCl	T6	-0.206	/	/
	T77	-0.202	/	/
	T76	-0.189	/	/
	T76 + T6	-0.187	/	/
20 mmol/L NaCl + 0.1 mol/L Na_2SO_4	T6	-0.168	0.069	0.237
	T77	-0.155	0.119	0.274
	T76	-0.143	0.173	0.316
	T76 + T6	-0.141	0.194	0.335
EXCO	T6	-0.049	/	/
	T77	-0.041	/	/
	T76	-0.04	/	/
	T76 + T6	-0.035	/	/

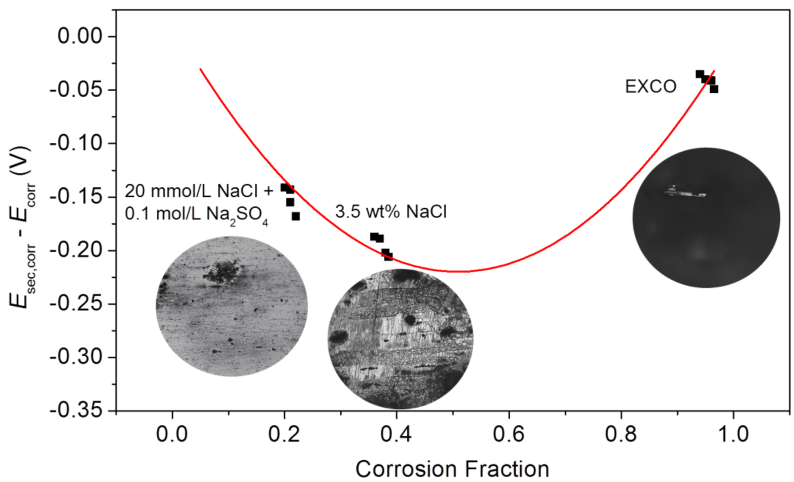

Figure 8. Schematic relationship of $E_{sec,corr} - E_{corr}$ and corrosion fraction of 7150 Al plate

Moreover, pitting potential and the related potential differences ($E_{pit} - E_{corr}$, $E_{pit} - E_{sec,corr}$) can be used to assess pitting corrosion [19], crevice corrosion [29] and SCC. The SCC susceptibility of 7150 Al plate subjected to various ageing treatments was characterized by the slow strain rate technique (SSRT) tests, as shown in Fig. 9 . The SSRT method was reported elsewhere [7]. The SCC indices, I_{SSRT}, calculated from SSRT curves, are compared with $E_{pit,2} - E_{corr}$ and $E_{pit,2} - E_{sec,corr}$ in Fig. 10. Surprisingly, an excellent agreement between the negative value of I_{SSRT} and potential differences was exhibited. This is due to that, both $E_{pit,2}$ and SCC of 7150 Al alloy are associated with the morphology and interspacing of grain boundary precipitates [13, 25, 30, 31]. $E_{pit,2} - E_{corr}$ is related with pitting corrosion initiation performance, while $E_{pit,2} - E_{sec,corr}$ is associated with pitting corrosion propagation ability. For 7000 series Al alloys, under applied or residual stress, SCC starts from pitting corrosion initiation on intergranular boundary, and then if pitting corrosion continues to propagate along the grain boundaries, the specimen would break down. Thus, the SCC resistance is proportional to the value of $E_{pit,2} - E_{corr}$ or $E_{pit,2} - E_{sec,corr}$, implying that SCC can be quickly assessed by these potential differences obtained by electrochemical methods.

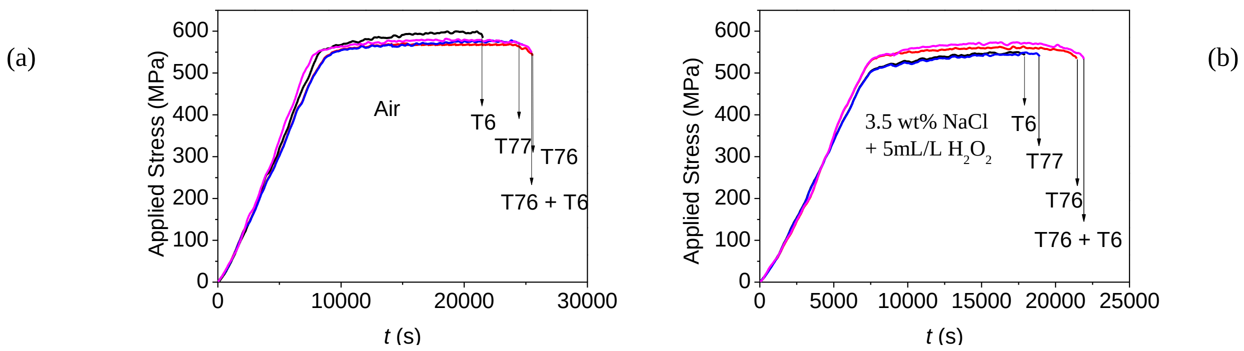

Figure 9. SSRT curves of 7150 Al alloys with different aging processes in different media: (a) air; (b) 3.5 wt% NaCl + 5mL/L H_2O_2 solution

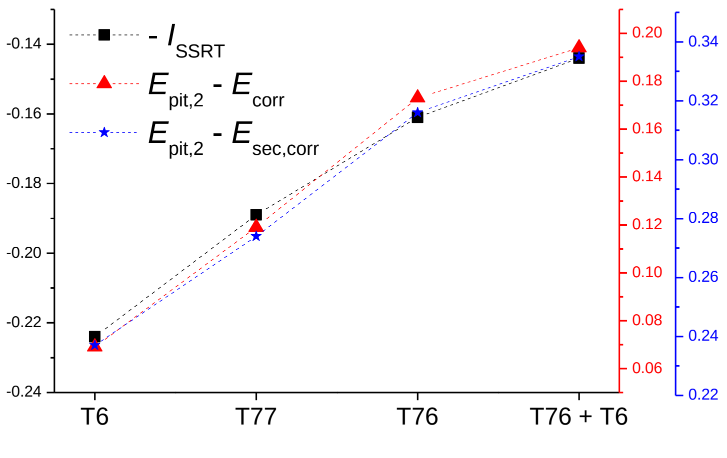

Figure 10. – I_{SSRT}, $E_{pit,2} - E_{corr}$ and $E_{pit,2} - E_{sec,corr}$ of 7150 Al plates subjected to T6, T77, T76 and T76 + T6 ageing treatments

4.4 Hardness and conductivity

As revealed by electrochemical measurements and SSRT tests, the novel three-step ageing T76 + T6 showed the best localized corrosion and SCC resistance. However, the increase in corrosion resistance of ultra-high strength Al–Zn–Mg-Cu alloys often is accompanied by the decrease in yield strength. In order to further study the feasibility of this novel ageing process, the hardness and conductivity values was compared with other tempers, as shown in Fig. 11. Compared to peak ageing T6, decrease of hardness was observed in all other tempers, among which over-aged temper T76 shows the largest decline. The hardness of RRA T77 and three-step ageing T76 + T6 is 179 Hv and 180 Hv, respectively. The approximation of hardness and better corrosion resistance prove that this novel three-step ageing (T76 + T6) process can be an alternative to the conventional RRA T77 ageing treatment, especially applicable for thick Al plates due to its longer regression time that can reduce residual stress problem. The electrical conductivity according to decreasing order is: T6 < T77 < T76 < T76 + T6, which implies that the SCC resistance also follows this order [32].

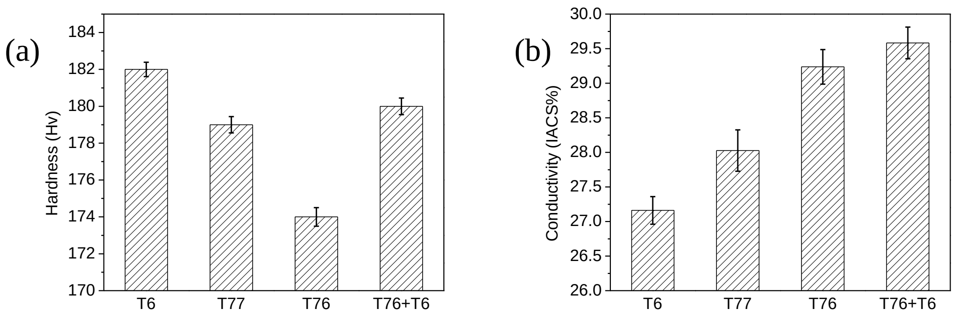

Figure 11. Hardness (a) and conductivity (b) of 7150 Al plates subjected to various ageing processes

4.5 TEM microstructure

The TEM microstructures of 7150 Al alloy plates subjected to various tempers are shown in Fig. 12. It is acknowledged that the strength of 7000 series alloys is mainly controlled by intra-grain precipitates. The usual precipitation sequence of Al–Zn–Mg–(Cu) alloys can be summarized as [33, 34]: solid solution → GP zones → metastable η′ → stable η ($MgZn_2$), where G.P. zone (coherent with matrix) and η' (semi-coherent with matrix) play an important role on strength while η (incoherent) has little effect on the strength. It can be seen from Fig. 12a that, very fine intra-grain features are observed in the 7150-T6 Al plate. According to Rajan et al. [35], the GP zones predominantly populate the grain interior of AA7150-T6, suggesting that the AA7050-T6 was strengthened by GP zones. Wu et al. [36] studied the microstructures of Al–Zn–Mg–Cu C912 alloy, and found that in addition to GP zones, there also existed some fine η′ precipitates. For RRA T77, it is evident that its intra-grain precipitate structure is slightly coarser than that of the T6, and the particle density is also decreased (seen from Fig. 12b), therefore, leading to the decline of strength. The intra-grain micrograph of over aged T76 is the coarsest and is distributed by large η phases which are due to the long over-ageing time (Fig. 12c), which corresponds to its lowest strength value. For T76 + T6 aged alloy as shown in Fig. 12d, the intra-grain is similar with that of RRA T77. As a result, the strength of T76 + T6 aged alloy is close to that of T77 aged alloy.

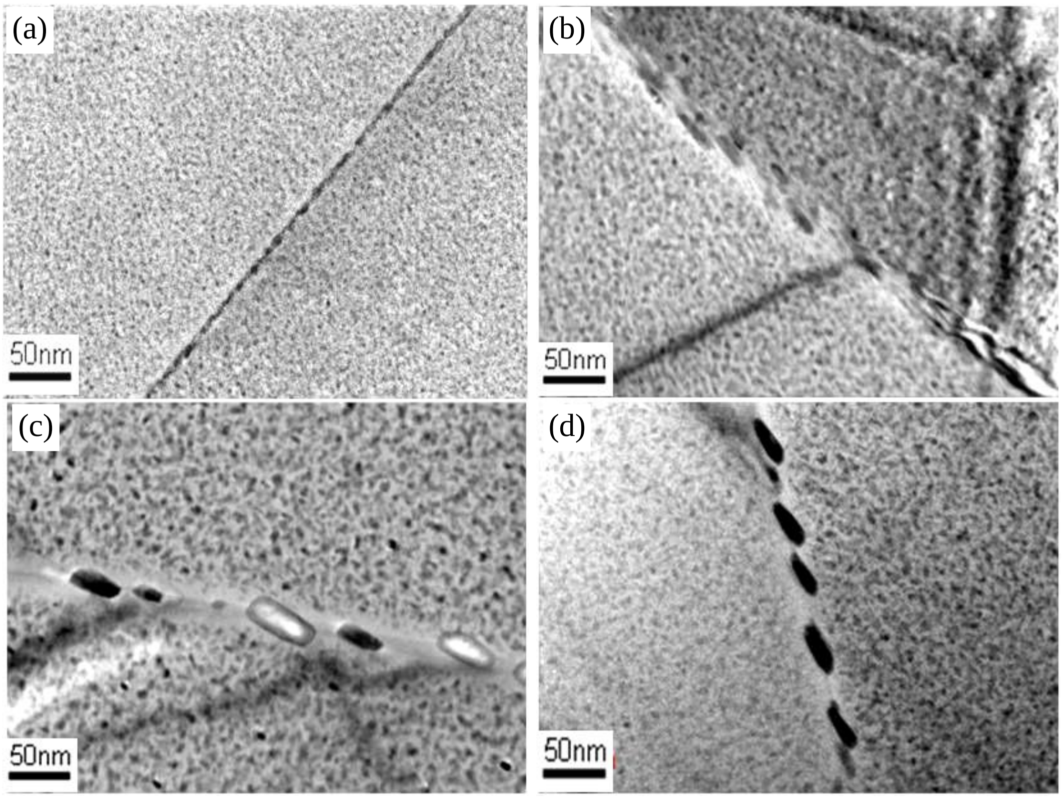

Figure 12. TEM microstructures of 7150 Al alloy plates subjected to various tempers: (a) T6; (b) T77; (c) T76; (d) T76 + T6

The corrosion performance of 7000 series Al alloy is associated with the distribution nature of grain boundary precipitates [2, 12, 37, 38]. The discontinuous distribution of the η precipitates at the grain boundary leads to the improvement of corrosion resistance, due to that it would cut off corrosion channel. The η precipitates are continuous or closely spaced at the grain boundaries in T6 aged 7150 Al alloy, implying a least localized corrosion resistance [39]. Compared with 7150-T6 Al alloy plate, the grain boundary η precipitates of the rest are coarser. Meanwhile, precipitate separation spacing is such that there is a clear discontinuous nature of the η precipitates for other ageing processes. Besides, the grain boundary indicated in Fig. 12d for the T76 + T6 tempered alloy is characterized by a larger size of the η intermetallics and by a higher interparticle spacing than for the RRA T77 temper. Therefore, T76 + T6 aged 7150 alloy shows a better localized corrosion resistance and SCC resistance than those of conventional 7150-T77 plate. In addition, recent research [40, 41] showed that the compositions of grain boundary precipitates also have large effect on localized corrosion and SCC behavior. Goswami et.al [42] observed considerable increase in Cu content in the grain boundary η in the over aged condition compared to the peak aged condition for 7075 Al alloy. They argued that the higher Cu content of the precipitate is associated with a lower SCC plateau velocity. Thus, whether microchemistry of GBPs or the discontinuity nature of GBPs plays a more important role on corrosion performance of 7000 series Al alloy is still unsettled. Further study concerning this would be needed.

5. CONCLUSIONS

(1) OCP and cyclic polarization results indicate that the localized corrosion resistance of alloys subjected to various tempers is in the following decreasing order: T76 + T6 > T76 > T77 > T6. Better corrosion resistance is associated with further coarsening and spacing of grain boundary precipitates as well as with higher Cu content of GBPs.

(2) Pit transition potentials (E_{ptp}) were obtained by plotting 2nd derivative curves of cyclic polarization curves. Though changed magnitude is relatively small, E_{ptp} has been proved to be a powerful criterion to assess repassivation behaviors of 7150 alloys subjected to various ageing conditions.

(3) Potential differences ($E_{pit} – E_{corr}$, $E_{pit} – E_{sec,corr}$) predict that the SCC resistance of the studied alloys is T76 + T6 > T76 > T77 > T6, which shows excellent agreement with slow strain rate technique results. This implies that electrochemical test under specific media can be an alternative to conventional time-consuming SCC analysis methods.

(4) There is suitability as well as limitations when using $E_{sec,corr} – E_{corr}$ for corrosion assessment. The value of $E_{sec,corr} – E_{corr}$ decreased firstly and then increased with the increasing of severity of corrosive medium.

ACKNOWLEDGEMENTS
The authors are happy to acknowledge financial support from Key Project of National Natural Science Foundation of China (No. 51134007), Project Major Research Equipment Development (51327902), National Basic Research Program of China (No. 2012CB619502, 2010CB731701), National Natural Science Foundation of China (No.51201186), and National key research and development program of China Study on Microstructure and mechanical properties of high performance aluminum alloy large size plate. The financial support of the China Scholarship Council is also gratefully acknowledged.

References

1. T. Dursun and C. Soutis, *Materials & Design*, 56 (2014) 862
2. H. Fang, H. Chao and K. Chen, *J. Alloys Compd.*, 622 (2015) 166
3. T. Warner. *Recently-developed aluminium solutions for aerospace applications*. in *Mater. Sci. Forum*. 2006. Trans Tech Publ.
4. M. Dixit, R. Mishra and K. Sankaran, *Materials Science and Engineering: A*, 478 (2008) 163
5. A. Oliveira, M. De Barros, K. Cardoso and D. Travessa, *Materials Science and Engineering: A*, 379 (2004) 321
6. B. Cina, *Reducing the susceptibility of alloys, particularly aluminium alloys, to stress corrosion cracking*. 1974, Google Patents.
7. G. Peng, K. Chen, S. Chen and H. Fang, *Materials Science and Engineering: A*, 528 (2011)

4014
8. F. Viana, A. Pinto, H. Santos and A. Lopes, *J. Mater. Process. Technol.*, 92 (1999) 54
9. Y.-P. Xiao, Q.-L. Pan, W.-B. Li, X.-Y. Liu and Y.-B. He, *Materials & Design*, 32 (2011) 2149
10. D. J. Chakrabarti, J. H. Goodman, C. M. Krist, J. Liu, R. R. Sawtell, G. B. Venema and R. W. Westerlund, *Aluminum alloy products having improved property combinations and method for artificially aging same*. 2005, Google Patents.
11. J.-Q. Su, T. Nelson, R. Mishra and M. Mahoney, *Acta Mater.*, 51 (2003) 713
12. H. Fang, K. Chen, X. Chen, H. Chao and G. Peng, *Corros. Sci.*, 51 (2009) 2872
13. Q. Meng and G. Frankel, *J. Electrochem. Soc.*, 151 (2004) B271
14. A. J. Bard, L. R. Faulkner, J. Leddy and C. G. Zoski, *Electrochemical methods: fundamentals and applications*. Vol. 2. 1980: Wiley New York.
15. C. Cao, *Principle of corrosion electrochemistry*. 2004, Beijing: chemical industry press.
16. M. Yasuda, F. Weinberg and D. Tromans, *J. Electrochem. Soc.*, 137 (1990) 3708
17. M. Finšgar and I. Milošev, *Corros. Sci.*, 52 (2010) 2430
18. I. M. Comotti, M. Trueba and S. P. Trasatti, *Surf. Interface Anal.*, 45 (2013) 1575
19. M. Trueba and S. P. Trasatti, *Mater. Chem. Phys.*, 121 (2010) 523
20. D. Cicolin, M. Trueba and S. Trasatti, *Electrochim. Acta*, 124 (2014) 27
21. K. Moore, J. Sykes and P. Grant, *Corros. Sci.*, 50 (2008) 3233
22. E. Melilli, M. Trueba and S. Trasatti, *La Metallurgia Italiana*, (2015)
23. M. Morrison, R. Buchanan, A. Peker, W. H. Peter, J. Horton and P. K. Liaw, *Intermetallics*, 12 (2004) 1177
24. D. Little, B. Connolly and J. Scully, *Corros. Sci.*, 49 (2007) 347
25. W. Zhang and G. Frankel, *Electrochim. Acta*, 48 (2003) 1193
26. S. Pride, J. Scully and J. Hudson, *J. Electrochem. Soc.*, 141 (1994) 3028
27. D. Silverman, *Uhlig's Corrosion Handbook, Third Edition*, (2011) 1129
28. D. C. Silverman, *Tutorial on cyclic potentiodynamic polarization technique*. 1998, NACE International, Houston, TX (United States).
29. B. Wilde and E. Williams, *Electrochim. Acta*, 16 (1971)
30. G. S. Peng, K. H. Chen, S. Y. Chen and H. C. Fang, *Mater. Corros.*, 64 (2013) 284
31. D. Wang, D. Ni and Z. Ma, *Materials Science and Engineering: A*, 494 (2008) 360
32. T. Tsai and T. Chuang, *Corrosion*, 52 (1996) 414
33. G. Sha and A. Cerezo, *Acta Mater.*, 52 (2004) 4503
34. K. Stiller, P. Warren, V. Hansen, J. Angenete and J. Gjønnes, *Materials Science and Engineering: A*, 270 (1999) 55
35. K. Rajan, W. Wallace and J. Beddoes, *Journal of Materials Science*, 17 (1982) 2817
36. Y. Wu, F. Froes, A. Alvarez, C. Li and J. Liu, *Materials & design*, 18 (1997) 211
37. S. Chen, K. Chen, G. Peng, L. Jia and P. Dong, *Materials & Design*, 35 (2012) 93
38. J.-f. Li, Z.-w. Peng, C.-x. Li, Z.-q. Jia, W.-j. Chen and Z.-q. Zheng, *Transactions of Nonferrous Metals Society of China*, 18 (2008) 755
39. J. F. Li, N. Birbilis, C. X. Li, Z. Q. Jia, B. Cai and Z. Q. Zheng, *Mater. Charact.*, 60 (2009) 1334
40. S. Knight, N. Birbilis, B. Muddle, A. Trueman and S. Lynch, *Corros. Sci.*, 52 (2010) 4073
41. T. Ramgopal, P. Gouma and G. Frankel, *Corrosion*, 58 (2002) 687
42. R. Goswami, S. Lynch, N. H. Holroyd, S. P. Knight and R. L. Holtz, *Metallurgical and Materials Transactions A*, 44 (2013) 1268